Influence of the Human Activity on the Propagation Characteristics of 60 GHz Indoor Channels

Sylvain Collonge, Gheorghe Zaharia, Ghais El Zein

Influence of the Human Activity on the Propagation Characteristics of 60 GHz Indoor Channels

Sylvain Collonge, *Student Member, IEEE*, Gheorghe Zaharia, and Ghais El Zein
Institute of Electronics and Telecommunications of Rennes (IETR) - UMR CNRS 6164
INSA - 20, av. des Buttes de Coesmes, 35043 Rennes, France
Email: sylvain.collonge@insa-rennes.fr

***Abstract*— The 60 GHz frequency band appears to be very promising for wireless multimedia services in the next years. The 60 GHz propagation channel has to be accurately characterized for an appropriate design of high data rate systems (>100 Mb/s). In this paper, our interest is to determine the influence of the human activity on the propagation characteristics at 60 GHz. This influence is hardly ever taking into account in the published studies on the 60 GHz channel characterization. However, the human activity is a determining factor at millimeter-waves. Channel sounding campaigns have been conducted. The measurement results highlight the strong disruptions caused by a person shadowing the direct path between two antennas. These disruptions make the channel unavailable for durations greater than 100 ms. Long-term measurements are analyzed in order to evaluate the "unavailability rate" of 60 GHz radio links. From these results, some solutions are suggested in order to reduce the shadowing problems.**

I. Introduction

The recent advances in wireless high data rate systems have conducted to explore higher frequency bands, such as the EHF band (Extremely High Frequency, 30-300 GHz). At these frequencies, propagation loss is strong, which is good for frequency reuse, and available bandwidths are large, which make it possible to ensure very high data rates (> 100 Mb/s). The applications under interest are often referred to as Fourth Generation or even Fifth Generation [1] of wireless communications. The channel characterization is an essential step in the design of these future systems, and particularly channel characterization based on measurements. Several published studies of the 60 GHz propagation focus on different aspects of the indoor channel: the influence of antennas directivity [2], [3], the influence of antennas polarization [4], the angles of arrival analysis [5], [6]. Nevertheless, the influence of the human activity on the propagation conditions is less analyzed. Yet, it is a critical aspect of the millimeter-waves propagation. The published studies rarely present measurement results ([7]: narrow band measurements at 30 GHz) but generally simulation results [8]-[10].

This paper presents 60 GHz wideband propagation measurements in the presence of a "natural" human activity. This work is based on several hours recordings of the channel impulse response, within an indoor environment. Section II presents the measurement setup (procedure, equipment, site description). In section III, the data processing is introduced and in section IV, the results are presented and analysed. Then, the section V concludes this work.

II. Measurement Setup

A. Measurement Equipments

1) Channel Sounder: A 60 GHz channel sounder based on the sliding correlation technique [11] was used. This sounder evaluates the channel impulse response (IR) with a 2.3 ns temporal resolution and a 40 dB relative dynamic. The delay observation window can be adjusted up to 1 μs. This window was set to 80 ns for these measurements. As the sliding factor is also adjustable, the measurement duration of one impulse response can be adapted to the temporal variations of the channel. This duration was set to 1.6 ms.

2) Antennas: Four antennas were used: two horns and two patches. The horns have a 22.4 dB gain and a 12° half power beamwidth (HPBW) in azimuth, and about 10° in elevation. The patches have a gain of about 3 dB and a 60° HPBW both in elevation and azimuth. The vertical polarization was used. Three couples of antennas are defined for transmission (TX) and reception (RX):

- a horn at TX and RX (HH configuration);
- a patch at TX and a horn at RX (PH configuration);
- a patch at TX and RX (PP configuration).

B. Measurement Environments

Measurements were carried out within two indoor environments: a residential house (Fig. 1) and a large room in the IETR laboratory (Fig. 2). The house was furnished and inhabited. The buildings materials are mainly breeze blocks, plasterboards and bricks. The laboratory room is a working place with desk and computers. In the upper-left corner is the coffee-area where researchers usually take a break. So, a varied human activity can be observed in this corner of the room during precise moments of the day. The furniture is composed by a wooden table, chairs with metallic legs, a wodden cupboard, a refregirator and a microwave oven. The walls are made of breeze-blocks with plaster. Windows are set in the right-hand wall.

C. Measurement Procedure

Short-term measurements have been performed in the House, and long-term measurements in the Laboratory. Antennas positions are shown in Fig. 1 and Fig. 2. As far as the laboratory is concerned, we will focus on the TX1 position. Table I presents the characteristics of each position.

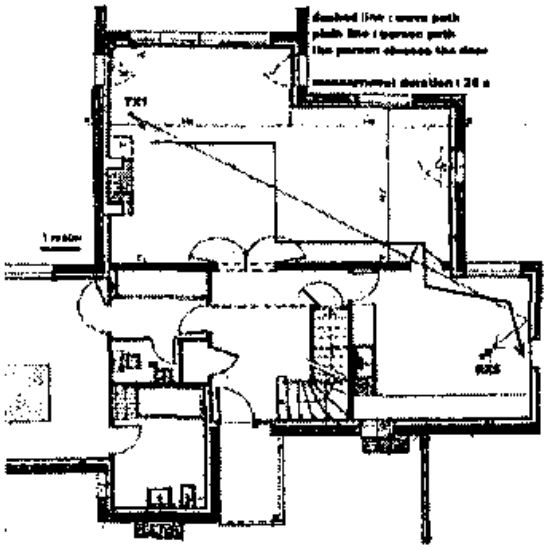

Fig. 1. Measurement site: House

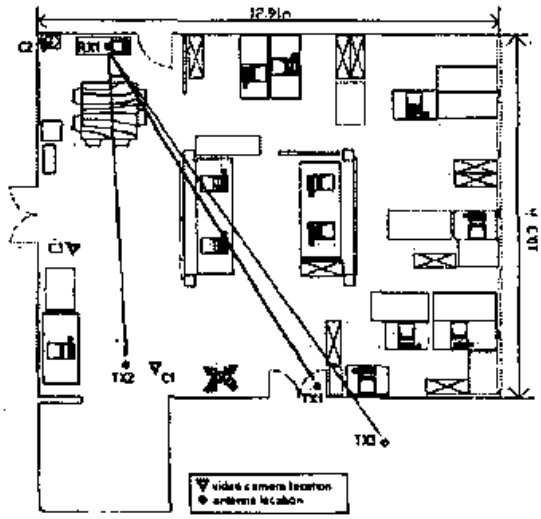

Fig. 2. Measurement site: Laboratory

For the measurements in the laboratory, RX and TX antennas were pointed at each other thanks to a laser pointer. For the measurements in the House, the antenna in TX1 was tilted toward the ground (15°). The antenna in RX5 has a nul elevation angle, and was pointed in azimuth to a wall from where an indirect path arrives from the door (as shown in Fig. 1).

For short-term measurements, impulse responses were stored during 25 seconds while a person moves within the environment, starting in the TX room and stopping in the RX room. When moving from one room to the other, at a speed of 1 m/s, the person closes the door (Fig. 1). This scenario is repeated for two heights of the TX antenna (patch, 2.20 m and 1.20 m) and for the two kinds of RX antenna (patch and horn).

Long-term measurements were performed over 15 days. Almost each day, a 40 minutes-long measurement was recorded at three moments, corresponding to coffee breaks: around 10:00, 13:00 and 16:00. Each day, TX position and antennas configurations were changed. During the measurements, a video camera shot the scene. Three camera positions were chosen, labeled C1, C2, and C3 in Fig. 2. The analysis of the video tapes makes it possible to know how many persons were in the neighborhood of the antennas. A varied human activity can be observed: between 0 and 15 persons, sitting and moving around the table, coming in and going out. Table II shows the measurement durations for the TX1 configuration.

TABLE I
CHARACTERISTICS OF TX AND RX POSITIONS

Environment	Position	Height	Visibility	Distance
Labs	RX1	1.55 m	LOS	10.8 m
	TX1	2.27 m		
House	RX5	1.20 m	NLOS	10.6 m
	TX1	2.20 m / 1.20 m		

TABLE II
MEASUREMENT DURATIONS (TX1, LABORATORY)

	0 pers.	1-5 pers.	6-10 pers.	11-15 pers.
HH1	55.2 min	141.0 min	62.2 min	5.8 min
PH1	33.0 min	92.0 min	56.4 min	14.9 min
PP1	22.7 min	112.6 min	21.9 min	3.6 min

III. DATA PROCESSING

A. Propagation characteristics

The channel sounder evaluates the complex IR: $h(\tau, t)$, where τ is the delay and t the time. From the IR, several propagation characteristics can be computed. To decrease the measurement noise level, the propagation characteristics are time-smoothed by means of a sliding window containing 9 temporal samples (12.8 ms). The median value within the sliding window is used to obtain the smoothed characteristics.

1) Attenuation: The attenuation $A(t)$ is the ratio of the transmitted power before the TX antenna on the received power after the RX antenna (the antennas are considered as parts of the channel). The transmitted and received powers are computed on the whole signal bandwidth.

2) Temporal fading: The temporal fading, $F(t)$, is the temporal variation of the attenuation around a reference level, A_{ref}.

$$F(t)_{[dB]} = A(t)_{[dB]} - A_{ref[dB]}$$

The reference level is measured before each long-term acquisition, when nobody is present. One can note that the median value of $A(t)$ is very close to the reference level.

B. Shadowing events

1) Definition: From the measurements, it can be observed (Fig. 3) that the attenuation strongly increases when the direct path is shadowed by a person. Series of sharp attenuation peaks

can be observed on the temporal evolution of the attenuation. These attenuation peaks are not uniformly distributed in time. This process is non-stationary because of people's movements.

We introduce the notion of "shadowing event" (SE) to characterize these attenuation peaks in amplitude and duration. A SE is detected when $F(t)$ becomes greater than a threshold. We used four threshold values: 5, 10, 15 and 20 dB. The begining of a SE, Tb_{SE} (respectively the end of a SE, Te_{SE}), is the instant of a threshold crossing with a positive (respectively negative) slope. To avoid taking into account small oscillations around the detection threshold, the calculation rules for Tb_{SE} and Te_{SE} are completed by a criteria on a minimal crossing duration and amplitude. Thanks to these conventions, the detected SEs globally fit with an intuitive detection of significant crossings. The SEs characteristics are the following (Fig. 3):

- duration: $D_{SE} = Te_{SE} - Tb_{SE}$
- mean amplitude:

$$A_{SE} = \frac{3}{D_{SE}} \int_{Tb_A}^{Te_A} F(t)dt$$

where:

$$Tb_A = Tb_{SE} + \frac{D_{SE}}{3} \quad \text{and} \quad Te_A = Te_{SE} - \frac{D_{SE}}{3}$$

A_{SE} is an average value computed over a time window centered on the middle of the SE. The width of this window is set to $\frac{D_{SE}}{3}$ to eliminate the contribution of the lateral sides of the attenuation peak.

- SE pseudo-period: I_{SE}

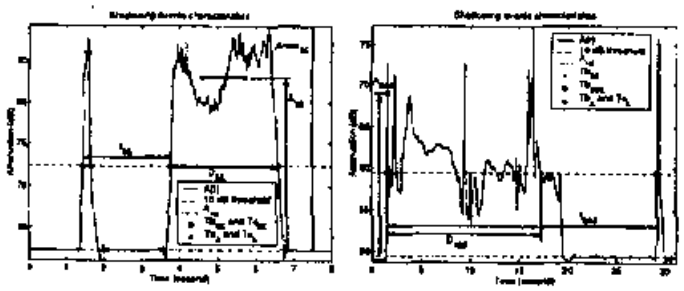

Fig. 3. SE and SSE characteristics (left: SE characteristics, right: SSE characteristics)

2) Series of shadowing events: The duration between successive SEs can be very short. These close SEs are generally caused by the movement of only one person between the antennas, as we noticed thanks to the video recordings. Moreover, the attenuation often stays greater than A_{ref} between two close SEs. To study this phenomenon, we define the notion of "series of shadowing events" (SSE). Two successive SEs, numbered n and $n+1$, belong to the same SSE if one of the following criteria is verified:

$$Tb_{SE}(n+1) - Te_{SE}(n) < t_{max}$$

or

$$\min_{t \in [Te_{SE}(n), Tb_{SE}(n+1)]} [F(t)] > A_{ref} + A_{margin}$$

After some adjustments, t_{max} is set to 1.5 seconds, and A_{margin} to 1 dB. Thanks to these definitions, a SSE closely corresponds to the physical interaction between a person and a wave path, as it can be seen on the video recordings. The SSE characteristics are the followings (Fig. 3):

- the number of SE per SSE: N_{SE}
- the begining and the end of the SEE:

$$Tb_{SSE} = Tb_{SE}(1) \qquad Te_{SSE} = Te_{SE}(N_{SE})$$

- the SSE duration: $D_{SSE} = Te_{SSE} - Tb_{SSE}$
- the SSE amplitude: $A_{SSE} = \max_{n=\overline{1,N_{SE}}}\{A_{SE}(n)\}$
- the SSE pseudo-period:

$$I_{SSE}(n) = Tb_{SSE}(n+1) - Tb_{SSE}(n), \quad n \geq 1$$

IV. Results and Discussion

A. Short-term measurements

Figure 4 shows $A(t)$ for the short-term scenarios. When the TX antenna is as high as the RX one (1.20 m), one can observe a SSE each time the person crossed the main path (shown in Fig. 1). On the other hand, when the TX antenna is close to the ceiling (2.20 m) the waves propagate above the person and there are no more SSEs. Around the 17-18th second, the person closed the door. From this moment, the attenuation increases by about 15 dB.

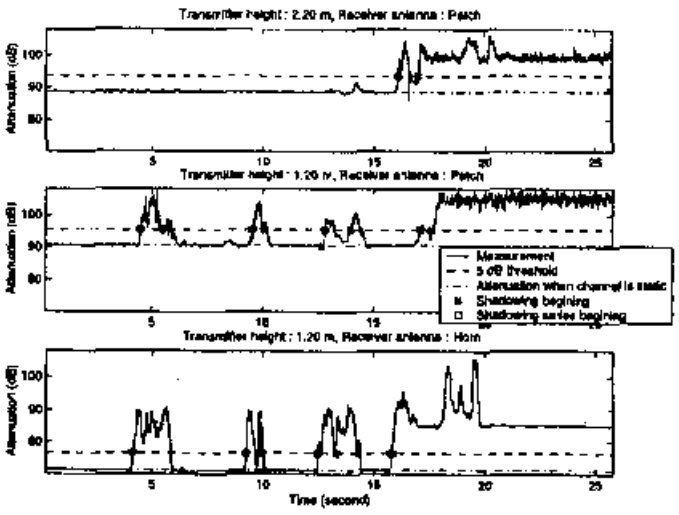

Fig. 4. House. TX1/RX5. Temporal evolution of the attenuation while a person walks and closes a door.

The SSE analysis is carried out for the part of the acquisition before the door was closed. The SSE characteristics are presented in Table III. One can notice that the phenomenon is stronger in duration and amplitude when the horn is used.

It can be noted that when the patch is used, the received power is low. When a SE happens, the received power level corresponds to the noise level. The SEs amplitude evaluation is then limited by the measurement dynamic. When the horn is used, the received signal level is higher and this limitation does not occur; therefore the measured amplitude is greater.

TABLE III

HOUSE. TX1/RX5. SSES CHARACTERISTICS

	Antenna	SSE 1	SSE 2	SSE 3
SSE Duration	Horn	1.722 s	0.772 s	1.888 s
	Patch	1.380 s	0.630 s	1.532 s
SSE Amplitude	Horn	13.2 dB	16.4 dB	16.5 dB
	Patch	10.7 dB	10.5 dB	7.9 dB

B. Long-term measurements

In this section, the same results are presented with respect to the human activity, which is quantified by the number of persons present in the neighborhood or between the antennas. As it is impossible to collect enough data for each number of persons from a natural activity, the analysis focuses on the following activity brackets: 0, 1 to 5, 6 to 10 and 11 to 15 persons. Table II shows the available duration of each activity bracket for all antennas configurations. For an activity of 11-15 persons, the observation durations are quite short (less than 15 minutes) to have statistically pertinent results.

1) SSE durations: Fig. 5 shows that there is no obvious dependence of the SSEs duration upon the antennas configuration. The SSE duration increases roughly linearly (on the logarithm scale) with the human activity. This exponential behavior can be explained by the combining of individual actions, increasing the number of SEs per SSE and therefore the SSE durations. The following "key figures" can be remembered for the median duration: 100 ms for 1 to 5 persons, 150 ms for 6 to 10 persons and 300 ms for 11 to 15 persons. The 90^{th} percentile of the SSE durations completes these figures and shows the spread of the duration values. More than a decade separates the median values from the 90^{th} percentiles.

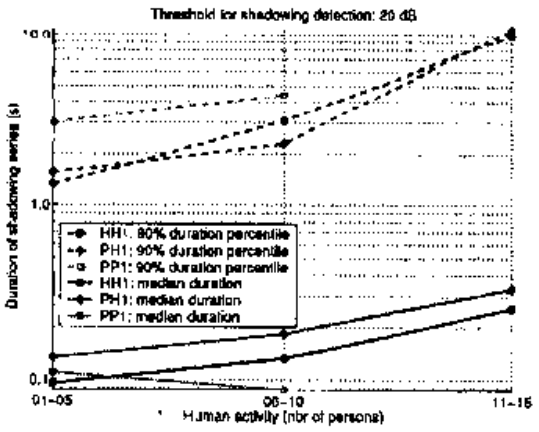

Fig. 5. Variations of the SSE durations for each antennas configuration

2) SSE amplitudes: The results show that the SSE amplitudes do not depend on the human activity. The mean SSEs amplitudes differ only from a maximum of 2 dB between an activity of 1-5 persons and an activity of more than 11 persons. Table IV shows the distribution of the SSE amplitudes for each antennas configuration. These values are extracted from the whole set of measurements (all activities are mixed up). The antennas configurations HH1 and PH1 reveal that the SSEs whose amplitude exceeds 20 dB are the most numerous (55.6% for HH1 and 78.2% for PH1). The mean amplitude of the SSEs detected with a 20 dB threshold is 23 dB. This is typical of a complete obstruction of the waves by a human body. The other amplitudes correspond to partial obstructions. The PP1 configuration has a different behavior than the two others. There are about 25% of the SSEs in each of the four amplitude categories. This can be explained by the antennas beamwidth: when the direct path is shadowed, indirect paths can reduce the SE amplitude.

TABLE IV

DISTRIBUTION OF THE SSE AMPLITUDES FOR EACH ANTENNAS CONFIGURATION

	5-10 dB	10-15 dB	15-20 dB	>20 dB
HH1	15.0%	10.5%	18.9%	55.6%
PH1	3.4%	3.9%	14.5%	78.2%
PP1	21.5%	22.1%	31.6%	24.8%

3) SSE pseudo-periods: The SSEs depend on the human activity. I_{SSE} spreads from about 2 seconds up to 5 minutes. Fig. 6 shows the median values for the HH1 configuration. I_{SSE} logically decreases when the human activity grows. The comparison between the different dectection thresholds reveals that when the number of persons within the environment is low (1-5), there is a diversity in the SSE amplitudes. This diversity decreases when the number of persons grows. The number of strong SSE amplitudes is higher when people are numerous.

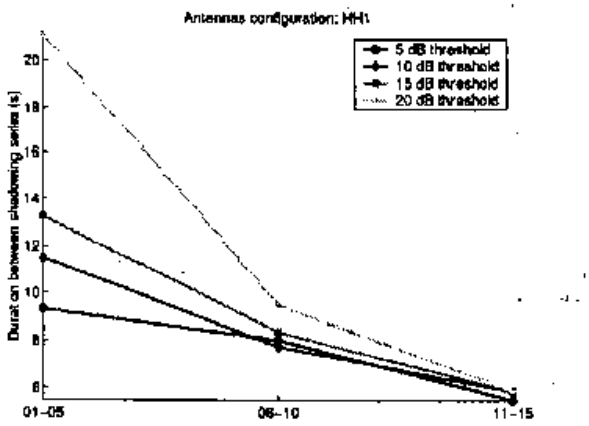

Fig. 6. Median values of I_{SSE} for HH1 configuration and all thresholds

4) Channel unavailability rate: One can reasonably think that the channel becomes unavailable during a series of shadowing events. The same observation is reported in [12] for 40 GHz radio links. From a communication system viewpoint, the shadowing events have three problematic characteristics: The fading rising time is very short, the fading duration is long, and the fading amplitude is strong. This means that every communication will be interrupted during a SE. The systems usually developped to overcome the channel temporal

variations will not be efficient in the case of the temporal variations of the 60 GHz channel. We define the channel "unavailability rate" (UR) as the sum of the SSE durations divided by the total measurement duration.

It is important to notice that the UR is highly dependant of the hazard of the human activity. A person can walk, stop on the direct path and stay there during a long time. 3.5% of all SSEs last more than 10 seconds and 1.0% more than 30 seconds. These very long SSEs can be seen as "outliers" and have a strong impact on the UR value. As these outliers are not uniformly distibuted between the antennas configurations and the human activity brackets, and as the observation times are not the same for all configurations, the comparisons might be distorted. A corrected UR is then computed so as each SSE with a duration that represents more than 0.5% of the total measurement duration, is not taken into account in the UR calculation. Fig. 7 shows the UR variation versus the human activity.

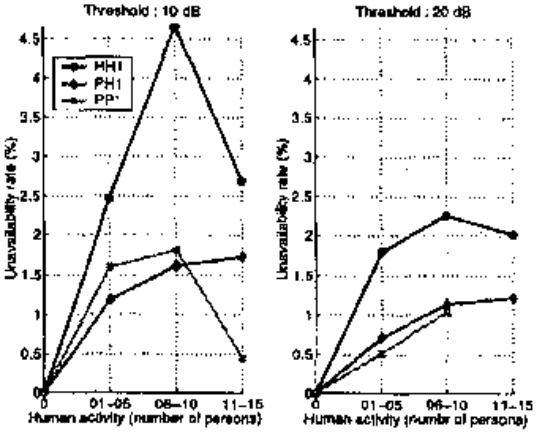

Fig. 7. Unavailability rate for 10 dB and 20 dB thresholds (TX1)

The UR increases with the human activity. The UR values are low for an activity of 11 to 15 persons because the observation durations are too short. One can underscore the effect of the antennas. Patch antennas can benefit from an angular diversity. Wave paths, sometimes created by moving persons, can be received from different directions of arrival, which reduces the shadowing phenomenon.

V. Conclusion

This work presents measurement campaigns of the 60 GHz propagation for time-varying channels. The temporal variations of the channel are caused by people's movements while antennas are fixed. The human bodies are significant obstacles for the millimeter-waves propagation. Some new definitions are introduced to quantify the impact of human activity on propagation characteristics. The results underline the duration and the amplitude of the shadowing effect caused by the human body. This leads to consider that the channel is unavailable during a shadowing event.

High data rate networks need to take into account this obstruction. Some solutions have been suggested by different authors. All these solutions take advantage of a sort of diversity. An access point diversity is often proposed [9], [10]. A disadvantage of such solutions is the amount of cabling and others network deployment considerations. Previous measurement campaigns revealed a diversity of the waves directions of arrival [13]. This diversity can be used to overcome the shadowing events. Actually, when a direction of arrival is obstructed by a human body, others are likely to be free. Multi-sector antennas associated with switching or combining systems must be developed to achieve this angular diversity. Moreover, if a device within the wireless network can be used for relaying the communications between two others, a sort of site diversity is added and obstruction problems are reduced again. The network deployment is simplified but, on the other hand, the modem complexity increases.

References

[1] S. Ohmori, Y. Yamao, and N. Nakajima, "The future generations of mobile communications based on broadband access technologies," *IEEE Commun. Mag.*, pp. 134–142, Dec. 2000.

[2] T. Manabe, Y. Miura, and T. Ihara, "Effects of antenna directivity and polarization on indoor multipath propagation characteristics at 60 GHz," *IEEE J. Select. Areas Commun.*, vol. 14, pp. 441–448, Apr. 1996.

[3] J.-H. Park, Y. Kim, Y.-S. Hur, K. Lim, and K.-H. Kim, "Analysis of 60 GHz band indoor wireless channels with channel configurations," in *Proc. IEEE International Symposium on Personal, Indoor and Mobile Radio Communications (PIMRC'98)*, Boston, Massachusetts, Sept. 8–11, 1998, pp. 617–620.

[4] T. Manabe, K. Sato, H. Marsuzawa, K. Taira, T. Ihara, and Y. Kasashima, "Polarization dependence of multipath propagation and high-speed transmission characterisitics of indoor millimeter-wave channel at 60 GHz," *IEEE Trans. Veh. Technol.*, vol. 44, pp. 268–274, May 1995.

[5] H. Xu, V. Kukshya, and T. Rappaport, "Spatial and temporal characterization of 60 GHz indoor channels," *IEEE J. Select. Areas Commun.*, vol. 20, pp. 620–630, Apr. 2002.

[6] S. Guerin, C. Pradal, and P. Khalfa, "Indoor propagation narrow band and wide band measurements around 60 GHz using a network analyser," EURO COST, Apr. 1995.

[7] P. Marinier, G. Delisle, and C. Despins, "Temporal variations of the indoor wireless millimeter-wave channel," *IEEE Trans. Antennas Propagat.*, vol. 46, pp. 928–934, June 1998.

[8] S. Obayashi and J. Zander, "A body-shadowing model for indoor radio communication environments," *IEEE Trans. Antennas Propagat.*, vol. 46, pp. 920–927, June 1998.

[9] M. Flament and M. Unbehaun, "Impact of shadowing fading in a mm-wave band wireless network," in *Proc. International Symposium on Wireless Personal Multimedia Communications (WPMC'2000)*, vol. 1, Bangkok, Thailand, Nov. 2000, pp. 427–432.

[10] K. Sato and T. Manabe, "Estimation of propagation-path visibility for indoor wireless LAN systems under shadowing condition by human bodies," in *Proc. IEEE Veh. Technol. Conf. (VTC'98)*, Ottawa, Ontario, Canada, May 1998, pp. 2109–2113.

[11] S. Guillouard, G. El Zein, and J. Citerne, "High time domain resolution indoor channel sounder for the 60 GHz band," in *Proc. European Microwave Conference (EMC'98)*, vol. 2, Amsterdam, The Netherlands, Oct. 1998, pp. 341–344.

[12] R. Bultitude, R. Hahn, and R. Davies, "Propagation considerations for the design of an indoor broad-band communications system at EHF," *IEEE Trans. Veh. Technol.*, vol. 47, no. 1, pp. 235–245, Feb. 1998.

[13] S. Collonge, G. Zaharia, and G. El Zein, "Wideband and dynamic characterization of the 60 GHz indoor radio propagation - future home WLAN architectures," Annals of Telecommunications, special issue on WLAN, Mar./Apr. 2003, to be published.